coatings

MDPI

Article

An Effectiveness Analysis for the Multi-Factor Accelerated Test of a Copper-Free Self-Polishing Antifouling Coating

Meng Chang [1,*], Junwei Jia [1], Congshu Huang [2], Shaonan Zhang [1], Lirong Tang [2], Lingling Jiang [1], Haoyuan Ma [1], Hao Lang [1], Qingqing Wang [1] and Jiashuo Yan [1]

[1] Beijing Orient Institute of Measurement & Test, Beijing 100086, China; jiajunwei@cast514.com (J.J.); zhangshaonan@cast514.com (S.Z.); 15010749436@163.com (L.J.); mahaoyuan@cast514.com (H.M.); langhaocn@163.com (H.L.); wangqq@cast.ntesmail.com (Q.W.); yjs19871202@126.com (J.Y.)
[2] Luoyang Ship Material Research Institute, Xiamen 361100, China; hcs05@126.com (C.H.); tanglrxm@163.com (L.T.)
* Correspondence: changmeng@cast514.com

Abstract: In order to eliminate or slow down the corrosion of various marine facilities, it has become a necessary choice to develop and use effective antifouling coatings for the development of marine equipment. This paper takes the newly developed copper-free, self-polishing, antifouling coating (CSAFC) as its research object, studies the performance changes in the exudation rate, adhesion, and abrasion rate by conducting a multi-factor accelerated test (MFAT) in the laboratory and a real sea test (RST), analyzes the correlation and acceleration multiplier in the two test environments, and provides a reference for the research on the relevant performance of this material. Firstly, it introduces the importance of antifouling coatings for modern maritime business, the importance of conducting accelerated tests in the laboratory, and explains the current test methods; secondly, it analyzes and fits the performance changes in materials such as the exudation rate, adhesion, and abrasion rate in different environments, and determines the main failure factors; finally, the correlation and acceleration multiplier are calculated using the Spearman rank correlation coefficient method (SRCCM) and acceleration factor method (AFM). The result shows that this MFAT has a good correlation and acceleration effect relative to the RST.

Keywords: corrosion; multi-factor accelerated test; correlation; acceleration rate

Citation: Chang, M.; Jia, J.; Huang, C.; Zhang, S.; Tang, L.; Jiang, L.; Ma, H.; Lang, H.; Wang, Q.; Yan, J. An Effectiveness Analysis for the Multi-Factor Accelerated Test of a Copper-Free Self-Polishing Antifouling Coating. *Coatings* **2023**, *13*, 1685. https://doi.org/10.3390/coatings13101685

Academic Editor: Giancarlo Galli

Received: 7 June 2023
Revised: 12 August 2023
Accepted: 14 August 2023
Published: 26 September 2023

1. Introduction

With the decrease in the Earth's resources and increasingly severe international competition, marine resources have become a competition point in the fields of resources, technology, and military for many countries. In recent years, various types of ships and submersibles have emerged and their application fields have been increasing, which provides great assistance for the development of marine resources. Seawater is a strong, corrosive medium composed of salt, microorganisms, oxygen, carbon dioxide, and microorganisms, etc. and combines waves, tides, currents, high pressures, low temperatures, and other environments [1–3], which will directly or indirectly accelerate the corrosion of equipment (Figure 1), seriously affect its safety and reliability, and enhance the cost of using and maintaining this marine equipment.

The application of antifouling coatings is one of the most effective technical methods of antifouling that is known to have been used. At present, antifouling coatings are widely used on the surfaces of ships and submersibles, which can not only reduce the formation of attached organisms and marine pollutants on the surfaces of ships, reduce the damage to the marine ecological environment, and improve the operation efficiency of ships, but also improve the service life of the surfaces of ships and submersibles and reduce the frequency and cost of their maintenance and repair [4–6]. In order to adapt to more severe

environments such as the deep sea and increase the durability of coatings to a greater extent, all types of coatings are constantly being upgraded.

Figure 1. Marine environmental hazards.

The development of coatings is a very long process, especially for the evaluation of antifouling performance. Traditional antifouling material tests are usually conducted in the actual application environment or a natural environment, which takes a considerable amount of time to complete, and if the performance test results of the coating do not match the expected results, the formulation needs to be readjusted to repeat the test [7]. Compared to the Natural Environment Test with a long period, an accelerated test in the laboratory can greatly speed up the time of the material performance verification, and more fully evaluate the performance of coating materials, which can facilitate the optimization of coating formulations and processes [8,9]. This paper will introduce and analyze the MFAT and the RST for the CSAFC.

2. Antifouling Coating

The main types of antifouling materials include traditional metal antifouling agent coatings, self-polishing antifouling coatings, low-surface-energy coatings, and modifications of low-surface-energy coatings [10–14]. Traditional metal antifouling agent coatings use metal fungicides to achieve the purpose of antifouling and generally fuse the fungicidal substances into some soluble or insoluble compound matrix, such as TBT-SPC coatings, which are extremely destructive to the ocean. Self-polishing antifouling coatings are hydrolyzed in seawater and self-polished by water currents, and marine fouling organisms attached to the coating surface are removed together with the copolymer film, which can control and regulate the leaching rate of biocides, typically represented by zinc-based acrylate copolymer coatings. Low-surface-energy coatings are different from traditional metal antifouling agent coatings, as they do not release any toxic substances into seawater, which meets the environmental goals of cleanliness and non-pollution, and due to their poor adhesion, marine fouling organisms are difficult to adhere to or can be easily removed by the impact of water. At the same time, they require additional costs and operating time to be used in conjunction with other coatings, typically represented by polydimethyl siloxane (PDMS). In addition, modified methods for low-surface-energy coatings are also being studied for their advantages and disadvantages, with the purpose of improving the adhesion, mechanical strength, and static antifouling ability for substrates, and mainly include nanocomposites, amphiphilic coatings, and non-toxic antifouling agent coatings, etc. [10].

This paper focuses on CSAFC, which is mainly based on zinc acrylate self-polishing resin and rosin, with the addition of zinc dextran, isothiazolinone, zinc pyrithione, TCPM and other organic antifouling agents, and thixotropic agents. Zinc acrylate self-polishing resin and rosin are slowly hydrolyzed and dissolved in water to promote the smooth seepage of antifouling agents and play a stable antifouling effect. Organic antifouling agents improve the antifouling coating's broad-spectrum performance. Thixotropic agents adjust the viscosity and anti-sagging properties of the coating, dissolve the resin and rosin base material, and ensure that the coating has a suitable spraying viscosity. Table 1 shows the formulation of copper-free, self-polishing, antifouling paint. The antifouling material has an excellent corrosion resistance, sea life fouling prevention, chemical resistance, abrasion resistance, and weather resistance, which can effectively protect marine facilities from erosion and damage caused by seawater, sea air, and UV rays [15–17].

Table 1. Formulation of CSAFC.

Serial Number	Chemical Composition	Percentage (%)
1	Zinc acrylate resin	15~20
2	Plasticizers	2~4
3	Organic antifouling agent	20~40
4	Auxiliary antifouling agent	20~40
5	Pigments	1~2
6	Thixotropic agents	1~2
7	Xylene	10~15

The main performance parameters of antifouling coatings include their exudation rate, adhesion, and abrasion rate. The exudation rate refers to the rate of the solvent volatilization of the coating material after heat or moisture, which must be controlled within a certain range, otherwise it will lead to an uneven composition of the coating and reduce its anti-fouling ability [18]. Adhesion refers to the bonding force between the coating material and the substrate. The adhesion of the antifouling coating must be strong, otherwise it will lead to the coating peeling off and losing its antifouling function [19–21]. The abrasion rate refers to the loss rate of the coating material when suffering from wear or friction. The abrasion rate of the antifouling coating must be low, otherwise it will lead to the loss of the coating's antifouling function [22]. Failure of any one of the exudation rate, adhesion, or abrasion rate can be considered as coating failure. The research will focus on the analysis of these performance parameters for coatings in different environments.

3. Test Method

3.1. Environmental Test Classification

The environmental test is the activity carried out to ensure that the product in the whole life cycle of the service environment maintains its functional reliability, and is mainly divided into a natural environment test, actual use environment test, and laboratory environment test [23]. The natural environment test puts the product in direct exposure to a natural environment for a long time, in order to determine the impact of the natural environment on its process, which is usually carried out in various types of natural exposure fields. The actual use environmental test will be installed on a platform, and directly undergo the action of the platform environment when using the product, in order to determine its adaptability to the platform environment. The laboratory environmental test puts the product in an artificially generated climate, mechanics, and other environments, in order to determine the effect of these environments on it without changing the failure mechanism of the product. It can evaluate the reliability or life index of the product in a short period time. The performance of antifouling materials is examined by observing the performance changes in the natural environment, using natural and laboratory environments [24–29]. Yilong Liu of Xiamen Shuangrui Marine Coating Co., Ltd. (Xiamen, China) adopted three different immersion methods to examine the performance changes of antifouling materials

with different resin and antifouling agent contents, including simultaneous exposure to fresh water and air, alternating normal-temperature immersion and low-temperature drying, and full immersion in fresh water [30]. Jiangtao Xiang of the Southwest Institute of Technology and Engineering analyzed the aging mechanism, color difference, and gloss change law of a polyurethane coating and accelerated the test effect, which was achieved by carrying out a comprehensive accelerated test with a low-pressure environment and a low-pressure natural environment test [31].

3.2. Test Method

3.2.1. General Test Method

The test will place the antifouling coating samples in a natural environmental and laboratory environment, respectively, and observe and analyze the changes in the main parameters such as the coating exudation rate, adhesion, and abrasion rate during the test. The main failure factors will be determined by function fitting, while the correlation and acceleration multiplier of the two test methods will be calculated via SRCCM and AFM.

The samples are coated with zinc yellow primer, thick-slurry-modified epoxy antirust paint, connecting paint, and antifouling paint in sequence by air spraying on the surface of a 30–50 μm thick aluminum alloy substrate, with a specification of 250 mm × 380 mm × 3 mm. The performance test data recorded each time are the average of multiple sample locations.

3.2.2. RST Method

RST is one kind of natural environmental test, in which antifouling coating samples are placed on a floating shin in the shallow sea and immersed in the nearest seawater. The performance of the samples is tested every six months until the performance of the samples fails. The site is located in Xiamen, China, where the average water temperature is 20.9 °C, the dissolved oxygen concentration is 5.3 mL/L, the salinity is 27%, the pH value is 8.2, the average tide difference is 3.84 m, and the average flow velocity is 0.2 m/s, which is a typical subtropical marine climate with the characteristics of a very vigorous growth of marine organisms.

3.2.3. MFAT Method

MFAT is one kind of laboratory environmental test, which includes pressure alternation, temperature alternation, and dry and wet alternation. The pressure alternation simulates the process of an alternate rise and fall of the coating at different depths in seawater, the temperature alternation simulates the process of seawater temperature changes when it alternately rises and falls at different depths, and the dry and wet alternation simulates the process of alternate reciprocation in atmospheric and seawater environments.

In the MFAT, each cycle of pressure-alternating test from a normal water pressure is pressurized to a specific value, held for 5 min, and then returned to a normal water pressure; each cycle of temperature-alternating test from the lowest temperature is held for 6 h, then rises to the highest temperature at a certain rate, holds for 6 h, and then drops to the lowest temperature; and each cycle of wet and dry alternating test dehydrates for 12 h and immerses in seawater for 12 h. The entire test carries out 30 cycles of pressure alternation (about 1 day), 1 cycle of temperature alternation (about 1 day), and 3 cycles of wet and dry alternation (about 3 days). Then, the material is sampled for exudation rate, adhesion, and abrasion rate testing (about 9 days), for a total of about 14 days per sampling major cycle. The water used during the test is seawater, which is the same as the seawater used in RST. After each sampling test is completed, the next large cycle test is continued until the coating fails. The details of the test are shown in Figure 2.

In the antifouling coating performance test, an exudation rate below 10 μg/(cm^2·d), an adhesion degradation below 50% of the initial value, or an abrasion rate close to 0 is considered failure.

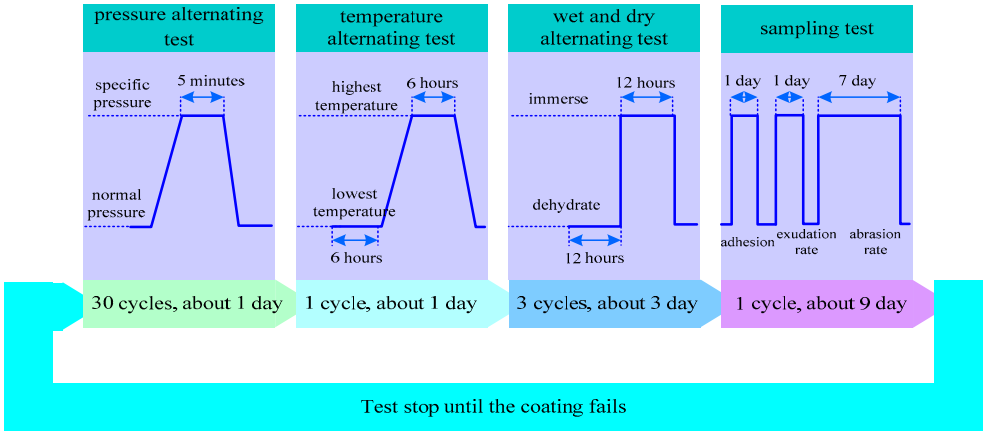

Figure 2. MFAT method process.

4. Analysis of Experimental Data

4.1. Data-Fitting Method

We establish a discrete data plot with the values of each performance parameter as vertical coordinates and the collection times as horizontal coordinates, which are based on the antifouling coating exudation rate, adhesion, and abrasion rate data obtained from each sampling. Then, we select the suitable fitting objective function and fit the discrete data using the Least Squares Method (LSM).

The LSM is a common data-fitting method that can be used to fit data with linear or nonlinear discrete patterns of variation. It can be used to impute unknown data easily by making the sum of the squares of the errors between these calculated data and the actual data minimal. The unknown value of its fitted objective function is obtained based on the given data set (x_i,y_i) (i = 1, 2, . . .n), which makes Equation (1) the minimum [32,33]. The objective functions used in this study mainly include the primary linear function and exponential decay function.

$$Q = \sum_{i=1}^{n} [y_i - \hat{y}_i]^2 = \sum_{i=1}^{n} [y_i - f(x_i)]^2 \quad (1)$$

where Q is the sum of squared residuals from the objective function and $\hat{y}_i$ is the value of the objective function in x_i.

4.1.1. Primary Linear Function

The primary linear objective function is given in the following Equation (2):

$$f(x) = ax + b \quad (2)$$

The values of the unknown parameters are calculated according to Equations (3) and (4):

$$b = \frac{\sum_{i=1}^{n} (x_i - \overline{x})(y_i - \overline{y})}{\sum_{i=1}^{n} (x_i - \overline{x})^2} \quad (3)$$

$$a = \overline{y} - b\overline{x} \quad (4)$$

where $\overline{x}$ is the arithmetic mean of x_1, x_2. . .x_n, and $\overline{y}$ is the arithmetic mean of y_1, y_2. . .y_n.

4.1.2. Non-Linear Exponential Decay Function

The exponential decay objective function is given in the following Equation (5):

$$f(x) = be^{ax} + c \quad (5)$$

It is difficult to find the minimum value of the residual sum of squares Q for nonlinear fitting functions sometimes, so we approximately linearize the nonlinear function by subjecting Q to Taylor expansion and then calculate the unknown parameters using iterative algorithms. Common optimization algorithms include the Fastest Descent Algorithm, Newton Algorithm, Guass–Newton Algorithm, and L m Algorithm, etc. [34]. It is optimized in a step-by-step procedure by resetting the x_k, Δk constantly, which makes $Q(x_k + \Delta k) < Q(x_k)$ until it converges to the limit. The L m Algorithm is an improved algorithm based on the Fastest Descent Algorithm and Guass–Newton Algorithm, whose iterative step is shown in Equation (6). When the damping coefficient u is large, the uI holds the dominant position, and then the L m Algorithm is equivalent to the Fastest Descent Algorithm; when the damping coefficient u is small, the approximate Hessian matrix $J(x)^T J(x)$ holds the dominant position, and then the L m Algorithm will be approximated as the Guass–Newton Algorithm [35].

$$\Delta x = -\left[J(x)^T J(x) + uI\right]^{-1}\left[J(x)^T f(x)\right] \tag{6}$$

where $J(x)$ is the Jacobian matrix of $f(x)$, I is the unit matrix, and u is the damping coefficient.

4.2. Data Analysis

4.2.1. Exudation Rate

Figure 3 shows the exudation rate data collected at each sampling moment in the laboratory MFAT (see black dots, each sampling data are the average of three sampling positions) and the function model fitted to these data (see red curve), with the black dots being connected to easily visualize the fitting effect of the data. The exudation rate kept decreasing with time and reached 7.9 μg/(cm^2·d) on day 280, which was lower than the failure criterion of 10 μg/(cm^2·d), and then the MFAT stopped. We fitted the collected data to predict the change in the exudation rate at each moment. After analysis, the change in the exudation rate with regard to time was relatively consistent with the nonlinear exponential decay function. Due to the large fluctuations in data changes from day 14 to day 42, which led to a poor fit of the data, we selected the data collected after day 42 and obtained the fitting function Equation (7).

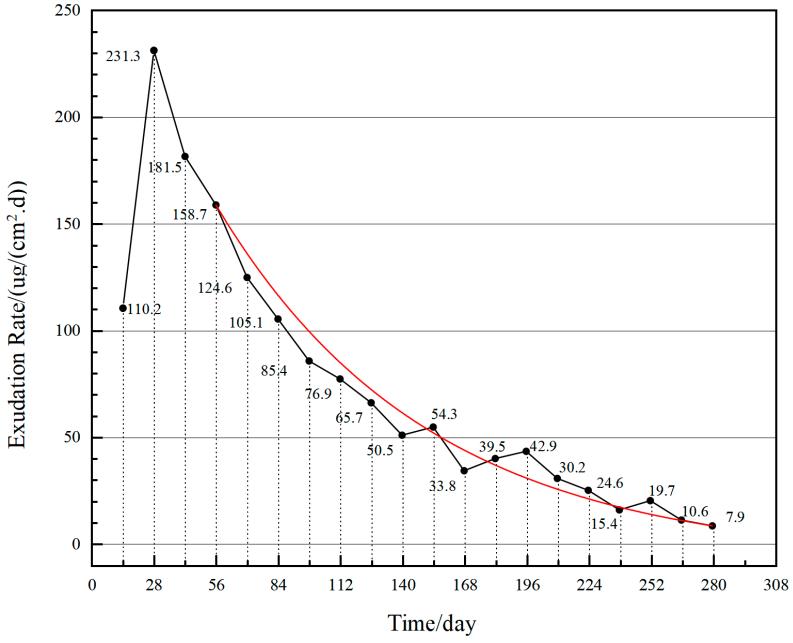

Figure 3. MFAT exudation rate change curve. The black curve represents the concatenation of the exudation rate data collected at each sampling moment in the laboratory MFAT, and the red curve represents the functional model fitted to these data.

According to the data, the rate of zinc exudation rose before day 28 at the beginning of the test, fell sharply from day 28 to day 42, tended to fall steadily from day 56 to day 168, and fell slowly from day 168 to day 280 until it was stabilized. Initially, the surface of the coating was mainly wrapped by resin components, which needed to be consumed by hydrolysis or seawater scouring to open the channel for the exudation of an antifouling agent, and the exudation rate was in a rising state. With the opening of the exudate channel, the resin was continuously hydrolyzed and abraded, and the new interface of the antifouling paint was continuously exposed; thus, the exuded zinc was continuously replenished, which could maintain a high exudate concentration at the beginning of the test. As the test time increased, the path of the zinc exudation was extended, the hydrolysis of the resin base material and zinc exudation reached a certain equilibrium state, and the rate of the zinc exudation tended to be stabilized. It could be seen that, by strengthening the strength and adhesion of the resin material, the breakage time of the resin base material could be slowed down, and the effective action time of the zinc exudation rate could be extended to a greater extent.

$$y = 299.93e^{-\frac{t}{95.35}} - 8.01 \quad (7)$$

4.2.2. Adhesion

Figure 4 shows the adhesion rate data collected at each sampling moment in the laboratory MFAT (see black dots, each sampling data are the average of seven sampling positions) and the function model fitted to these data (see red curve), with the black dots being connected in order to easily visualize the fitting effect of the data. The degradation of the adhesion performance had an obvious linear decreasing trend, and the adhesion force was always higher than 50% of the initial adhesion force until the end of the test, with no failure. We used a linear function to fit it, and obtained the fitting function Equation (8) of the adhesion force with time change.

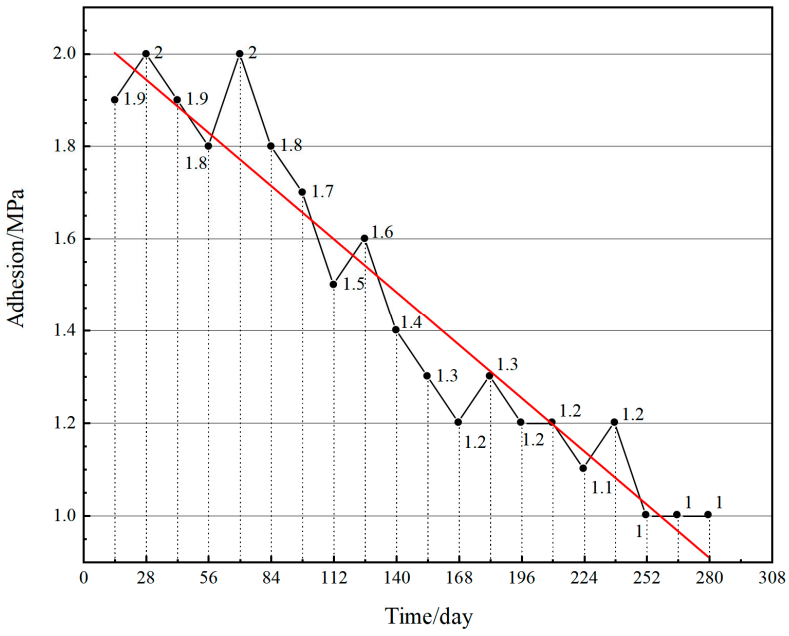

Figure 4. MFAT adhesion change curve. The black curve represents the concatenation of the adhesion data collected at each sampling moment in the laboratory MFAT, and the red curve represents the functional model fitted to these data.

The coating's adhesion depends on mechanical bonding, physical adsorption, the formation of hydrogen and chemical bonds, mutual diffusion, and other effects of bonding between the paint film and the substrate. According to the data, the adhesion was in a fluctuating decline from the beginning until it reached a steady state on day 252, where it

then remained until day 280. The resin was continuously hydrolyzed from the beginning to the middle and late stages of the test, which caused changes in the mechanical bonding and physical adsorption state, etc. and decreased the adhesion. After the hydrolysis of the resin was balanced at the end of the test, the adhesion was stabilized. It could be seen that the resin has a very strong influence on the adhesion, which is an important factor in determining the peeling of coatings.

$$y = -0.004t + 2.059 \quad (8)$$

4.2.3. Abrasion Rate

Figure 5 shows the abrasion rate data collected at each sampling moment in the laboratory MFAT (see black dots, each sampling data are the average of three sampling positions), with the black dots being connected in order to facilitate a more intuitive view. The abrasion rate did not have an obvious pattern and fluctuated in the range from 5.4 μm to 10.8 μm every month, which did not reach the failure state. There was no way to create a fitting function for it. According to the data, the abrasion rate fluctuated around the average value, which indicates that the resin hydrolysis and polishing were relatively stable.

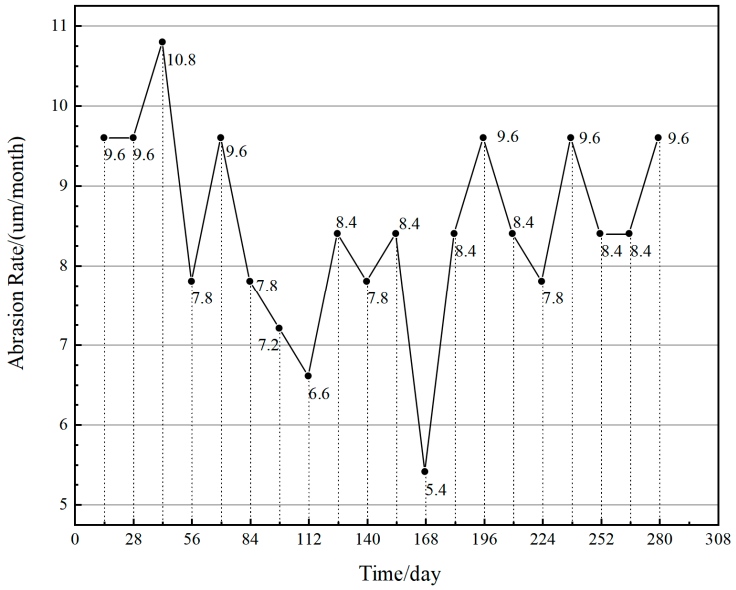

Figure 5. MFAT abrasion rate change curve.

5. Evaluation Validation

5.1. Correlation Verification

5.1.1. Verification Method

Correlation validation is the process of verifying the relationship between two or more variables, which is an important indicator of the relationship between the accelerated test and the actual application environment. The correlation coefficient is usually used to measure the intensity and direction of the relationship between variables. The correlation coefficient takes values in the range from −1 to 1, in which −1 means a completely negative correlation, 0 means no correlation, and 1 means a completely positive correlation. The main methods for correlation validation include the Pearson product-moment correlation coefficient method, SRCCM, and Gray correlation analysis [36,37]. In this study, we used SRCCM to verify the correlation between the MFAT in the laboratory and the RST.

When the values of the main failure performance parameters of the coating reached L_1, $L_2 \ldots L_n$, the corresponding time lengths in the RST environment were T_{s1}, $T_{s2} \ldots T_{sn}$, which were ordered as x_1, $x_2 \ldots x_n$, and the corresponding time lengths in the laboratory MFAT

environment were T_{J1}, T_{J2}...T_{Jn}, which were ordered as y_1, y_2...y_n. The value of the rho_s was calculated using SRCCM, which is shown in Equations (9) and (10):

$$d_i = x_i - y_i \tag{9}$$

$$rho_s = 1 - \frac{6\sum_{i=1}^{n} {d_i}^2}{n^3 - n} \tag{10}$$

where d_i is the rank difference and n is the number of reference specimen groups.

5.1.2. Analysis of Results

According to the data analysis, the main failure factor of the selected coating was the exudation rate, and the exudation rate rank correlation coefficient of the RST historical data and the MFAT model is shown in Table 2.

Table 2. Exudation rate rank correlation coefficient.

Exudation Rate L_i (μg/(cm^2·d))	RST Time T_{si} (day)	RST Time Order x_i	MFAT Model Test Time T_{Ji} (day)	MFAT Model Test Time Order y_i	Rank Difference d_i
34.2	182	1	185	1	0
20.9	365	2	222	2	0
15.7	547	3	240	3	0
8.7	1080	4	276	4	0

5.2. Accelerated Multiplier

5.2.1. Verification Method

The acceleration multiplier is the ratio of the accelerated factor in the laboratory accelerated test environment to the accelerated factor in the actual application environment, usually expressed as a number, which is an important factor for evaluating the accelerated effect of an accelerated test. It can generally be calculated by the ratio of the time required for the same performance of the material to degrade to the same level in the accelerated test environment and in the actual application environment.

Acceleration evaluation methods generally include the AFM or acceleration switching factor method [38,39]. In this study, we will use the AFM to verify the acceleration effect, which is shown in Equation (11).

$$\alpha = \frac{T_2}{T_1} \tag{11}$$

where α is the acceleration multiplier, T_1 is the failure time of the material in the accelerated test environment, and T_2 is the failure time of the material in the RST environment.

5.2.2. Analysis of Results

Figure 6 shows the exudation rate data collected at each sampling moment in the RST (see black dots, each sampling data are the average of three sampling positions) and the function model fitted to these data (see red curve), with the black dots being connected in order to easily visualize the fitting effect of the data. The exudation rate decreased more and more slowly from day 180 to day 1080, until it stabilized. We selected nonlinear exponential modeling to obtain the fitting function Equation (12).

Compared with the MFAT, the zinc exudation rate in the RST did not show an initial increase, which was due to the fact that the exudation channel had been opened before the first sampling. Meanwhile, the zinc exudation rate was maintained at a lower level, which was mainly due to the fact that the test environment of the antifouling paint was at a higher seawater temperature in the MFAT, and favored the dissolution and diffusion of oxygen and the electrochemical dissolution of zinc. The final exudation rate of the zinc in both test

methods remained around 7–10 μg/(cm^2·d), which indicated that the exudation area of zinc is stable after a period of time, and the results of the two test methods were similar.

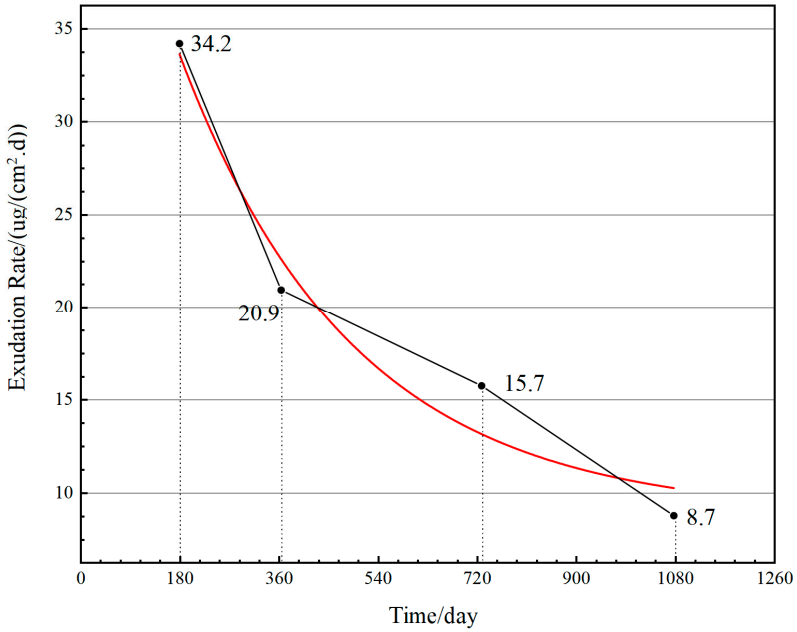

Figure 6. RST exudation rate change curve. The black curve represents the concatenation of the exudation rate data collected at each sampling moment in the RST, and the red curve represents the functional model fitted to these data.

According to the fitting function of the coating in the MFAT, the coating will fail on day 268 in the MFAT environment and fail on day 1033 in the RST environment. The acceleration multiplier was 3.85, which was obtained via the AFM and was bigger than the universal acceleration multiplier 3. Figure 5 shows the discrete data and fitting function of the exudation rate in the RST.

$$y = 41.576e^{-\frac{t}{457.11}} + 5.60 \quad (12)$$

6. Conclusions

This paper summarized and analyzed the process and results of MFAT and RST for CSAFC, and drew the following conclusions:

1. The LSM was successfully applied to the linear and exponential modeling of the test data, and degradation models were obtained for parameters such as the exudation rate and adhesion, through which the main failure factors and failure times of the antifouling coatings under different test environments were deduced.
2. The exudation rate is the main failure factor in both MFAT and RST, which shows a rapid decline and then tends to stabilize, and the failure mechanism is consistent.
3. The SRCCM and AFM were successfully applied to obtain the correlation coefficient and acceleration multiplier, confirming that the MFAT of copper-free, self-polished antifouling coatings has a good correlation and acceleration effect relative to the RST, which indicates that this MFAT is accurate and fast.

Author Contributions: Conceptualization, methodology, formal analysis, writing—original draft preparation, M.C.; validation, M.C. and L.T.; investigation, writing—review and editing, J.J.; resources, S.Z.; data curation, L.J., H.M. and J.Y.; visualization, Q.W.; project administration, C.H.; supervision, H.L. All authors have read and agreed to the published version of the manuscript.

Funding: This research received no external funding.

Institutional Review Board Statement: Not applicable.

Informed Consent Statement: Not applicable.

Data Availability Statement: Not applicable.

Conflicts of Interest: The authors declare no conflict of interest.

References

1. Pan, J.L.; Liang, H.Y.; Zhang, E.W.; Xi, X.Y. Research Progress on Mechanical Properties of Steel Under the Marine Corrosion Environment. *Corros. Res.* **2022**, *08*, 125–128.
2. Mao, H.B.; Wu, Y.T.; Yin, J.P.; Lian, S.M. Development Status and prospect of marine environmental security technology. *Bull. Chin. Acad. Sci.* **2022**, *7*, 870–880. [CrossRef]
3. Faÿ, F.; Champion, M.; Guennec, A.; Moppert, X.; Simon-Colin, C.; Elie, M. Biobased Anti-Adhesive Marine Coatings from Polyhydroxyalkanoates and Polysaccharides. *Coatings* **2023**, *13*, 766. [CrossRef]
4. Wu, B.; Lu, X.; Wang, Y.X.; Li, J.L.; Ye, Y.W.; Zhao, W.J. Tribological Behavior of TiN and TiSiN Coatings in Seawater. *Surf. Technol.* **2017**, *11*, 143–148. [CrossRef]
5. Fang, Y.H.; Zhou, K.H.; Cai, H.; Sun, L.S.; Liu, Z.W.; Wang, C.T.; Zheng, W.R.; Pu, J.B.; Liu, Q.; Li, Z. Effect of polarization potential on properties of copper-based antifouling coating. *Electropating Finish.* **2018**, *2*, 76–81.
6. Gevaux, L.; Lejars, M.; Margaillan, A.; Briand, J.-F.; Bunet, R.; Bressy, C. Hydrolyzable Additive-Based Silicone Elastomers: A New Approach for Antifouling Coatings. *Polymers* **2019**, *11*, 305. [CrossRef] [PubMed]
7. Deng, L.; Lin, C.G.; Zhang, J.W.; Ma, L.; Su, Y.; Cheng, X.D.; Shao, G.Q.; Wang, L. Service Life Model and Indoor Accelerated Evaluation Method of Fouling-release Coatings. *Surf. Technol.* **2022**, *5*, 293–303. [CrossRef]
8. Xu, B.; Liu, Q.; Qian, J.C.; Bai, Y.H.; Li, J.Y.; Fang, M. Protective Performance of Fluoropolyurethane Coating System in Simulated Marine Environment. *Surf. Technol.* **2022**, *9*, 243–250. [CrossRef]
9. Li, Q.; Li, J.Y.; Sun, M.J.; Hu, T.; Wang, L. Performance Degradation of Three Coatings in Simulated Tropical Marine Atmospheric Environment. *Environ. Test* **2023**, *3*, 11–16.
10. Song, C.X. Preparation and Properties of Silicone Marine Antifouling Coatings. Master's Thesis, Qingdao University of Science & Technology, Qingdao, China, 18 May 2022.
11. Liu, H.B.; Zhang, L.W.; Chen, W.J.; Chen, Y.M.; Shen, G.X.; Tang, C.Y.; Shao, D.X.; Zheng, D.M. Research Progress of Antifouling Coatings for Ships. *Shandong Chem. Ind.* **2023**, *52*, 240–242.
12. Niu, Y.F. Study on Freshwater Immersion Resistance of Ship Antifouling Coatings. *China Coat.* **2022**, *12*, 34–38.
13. Mo, Y.Q. Preparation and Properties Study of Bionic Low Surface Energy Antifouling Coatings. Master's Thesis, Dalian Maritime University, Dalian, China, 7 June 2022.
14. Guazzelli, E.; Oliva, M.; Pretti, C.; Monni, G.; Fahs, A.; Bressy, C.; Martinelli, E. Polyethylene Glycol-b-poly(trialkylsilyl methacrylate-co-methyl methacrylate) Hydrolyzable Block Copolymers for Eco-Friendly Self-Polishing Marine Coatings. *Polymers* **2022**, *14*, 4589. [CrossRef] [PubMed]
15. Wang, C.J.; Liu, S.P.; Wang, Z.H.; Luo, H.X. New Development of the Research and Applications of Antifouling Coatings. *Mater. Rep.* **2022**, *23*, 21020004. [CrossRef]
16. Deng, B.F.; Xie, Z.P.; Wang, J.J.; Tang, L.R. Research on Matching and Antifouling Performance of Zinc Acrylate Self-polishing Antifouling Paint. *Dev. Appl. Mater.* **2017**, *2*, 12–17.
17. Tao, L.; Yin, Z.P. Progress of Self-Polishing Antifouling Technology in Field of Marine Antifouling Coating. *Coat. Prot.* **2022**, *04*, 55–62.
18. Ding, R.; Jiang, J.M.; Gui, T.J.; Li, X.B. The Cu Leaching Rate of Cold Spray Copper Composite Coatings in Multivariate Marine Environment and Prediction System Based on BP Artificial Neural Network. *Exp. Res. Appl.* **2016**, *6*, 5–9.
19. An, J.L.; Wan, M.; Tang, S.; Huo, X.J. Study of Anti-Corrosion Performance and Adhesion of Tung Oil/Lanolin Microcapsule Coating. *Mater. Prot.* **2023**, *5*, 139–147.
20. Zhao, Y.Y.; Lu, W.Z.; Wu, B.J.; Sun, Y.L.; Zuo, D.W. Effects of Erosion Angle on CFRP Skin Coating Removal and Adhesion of Recoating. *China Surf. Eng.* **2023**, *1*, 116–123.
21. Shi, X.; Han, Q.; Chen, T.T.; Wang, W.M. Analysis of Factors Affecting Adhesion of Waterborne Paint for Casting. *Technol. Exp. Communion* **2023**, *1*, 31–36.
22. Xu, C.S.; Yao, J.H. Discussion of Polishing Rate Test for Self-Polishing Antifouling Coatings. *Paint. Coat. Ind.* **2016**, *2*, 70–74.
23. Xu, H. Discussion on Classification for Environmental Testing. *Trainer* **2014**, *4*, 65–68.
24. Deng, B.F.; Zhang, C.Y.; Huang, C.S.; Xie, Z.P.; Wang, J.J.; Hu, M.Y. Preparation and Performance Studies of Zinc Acrylateself-Polishing Copper-Free Antifouling Coatings. *Paint. Coat. Ind.* **2020**, *12*, 32–36.
25. Jin, Q.J.; Liang, T.; Lv, L.F.; Zhang, H.J.; Wang, Y. Study of the Evaluation of Anti-Corrosion Performance of Galvanized Materials by Different Corrosion Test Methods. *Mater. Prot.* **2023**, *2*, 51–56.
26. Gong, H.; Xu, C.Q.; Yao, J.h. Correlation Analysis for Copper Release Rate Test Results of Antifouling Paint in Indoor Simulated and Real Seawater Environment. *Dev. Appl. Mater.* **2022**, *12*, 114–118.
27. Wieberger, F.; Kolb, T.; Neuber, C.; Ober, C.K.; Schmidt, H.-W. Combinatorial Techniques to Efficiently Investigate and Optimize Organic Thin Film Processing and Properties. *Molecules* **2013**, *18*, 4120–4139. [CrossRef] [PubMed]

28. Carcione, F.; Defeo, G.A.; Galli, I.; Bartalini, S.; Mazzotti, D. Material Circularity: A Novel Method for Biobased Carbon Quantification of Leather, Artificial Leather, and Trendy Alternatives. *Coatings* **2023**, *13*, 892. [CrossRef]
29. Zhang, H.; Zhang, X.; Zhao, X.; Tang, Y.; Zuo, Y. Preparation of Ti–Zr-Based Conversion Coating on 5052 Aluminum Alloy, and Its Corrosion Resistance and Antifouling Performance. *Coatings* **2018**, *8*, 397. [CrossRef]
30. Liu, Y.L.; Wang, S.L.; Li, C.G.; Fang, D.Q.; Wu, J.H. Preparation and Performance of Environment-friendly Copper-free Self-polishing Antifouling Paints. *Surf. Technol.* **2017**, *12*, 1–5.
31. Xiang, J.T.; Yang, X.K.; Yang, X.R. Application of Comprehensive Accelerated Test Technology in Rapid Evaluation of Polyurethane Coating in Low Pressure Environment. *Equip. Environ. Eng.* **2021**, *12*, 128–133. [CrossRef]
32. Wang, H.J.; Cui, G.Y.; Fan, H.H.; Feng, W.H. Application of Least Square Method in Circuit Experiment. *J. Electr. Electron. Educ.* **2022**, *6*, 152–155.
33. Li, Z.P. Design of Voltage Detection Algorithm Based on Least Square Method. *Parts Des.* **2022**, *11*, 22–25.
34. Zhao, Y.X.; Liu, S.C.; Yan, W.; Zhu, Z.B.; Ju, M. Study on Modeling of Silicon Carbide MOSFET Based on Levenberg-Marquardt Algorithm. *J. Nanjing Norm. Univ. Eng. Technol. Ed.* **2022**, *3*, 30–37.
35. Xiao, S.R.; Hu, Q.C.; Li, N.N.; Chen, X.B. Research on multi-sensor calibration method of UAV based on Levenberg-Marquardt algorithm. *Mach. Tool Hydraul.* **2022**, *10*, 12–18.
36. Wang, J.F.; Li, X.; Yin, Z.L.; Yang, X.R. Application of Multi-factor Integrated Simulation of Marine Climate and Acceleration Test Technologies in Screening of Fastener Surface Treatment Technologies. *Surface Technol.* **2016**, *2*, 175–180.
37. Jia, K.; Yang, Z.; Wei, C.; Zheng, L.M.; Li, Y.B.; Bi, T.S. Pilot Protection Based on Spearman Rank Correlation Coefficient for Transmission Line Connected to Renewable Energy Source. *China Surf. Eng.* **2020**, *15*, 103–111.
38. Peng, J.C.; Guo, Z.H.; Yang, X.R. Relativity and Acceleration Verification of Multi-factors Integrated Marine Climate Natural Accelerated Test Technologies. *Equip. Environ. Eng.* **2016**, *5*, 98–104.
39. Chen, Z.C.; Li, H.S.; Zhang, P.S.; Zhou, Y.R. Highly Accelerated Ground Simulation Technology of Space Ultraviolet Radiation. *Equip. Environ. Eng.* **2021**, *2*, 57–61.